# Excitation spectrum and ground state properties of the $S = \frac{1}{2}$ Heisenberg ladder with staggered dimerization

V.N. Kotov[†], J. Oitmaa[‡], and Zheng Weihong[*]

*School of Physics, The University of New South Wales*

*Sydney 2052, Australia*

(February 1, 2008)

## Abstract

We study the excitation spectrum and ground state properties of the two-leg $S = \frac{1}{2}$ quantum spin ladder with staggered dimerization. Two massive phases, separated by a critical line are found, as predicted by previous analysis, based on the non-linear sigma model (NLSM). We have used dimer series expansions, exact diagonalization of small clusters and diagrammatic analysis of an effective interacting Bose gas Hamiltonian, obtained by using the bond operator representation for spins. We compute the excitation spectrum in the phase, dominated by strong rungs in the parameter regimes far away and close to the point of instability. The exact location of the phase boundary is determined.

75.10.Jm, 75.30.Ds, 75.40.Gb, 75.30.Kz

# I. INTRODUCTION

There is a great deal of current interest in quasi one-dimensional quantum spin models, such as spin ladders, spin chains with dimerization and (or) frustration, and various generalizations of the above. The studies of these models have been mostly triggered by the experimental discoveries of several spin-Peierls and spin-ladder compounds [1]. The theoretical efforts have been focused mainly on the nature of the ground state, the excitation spectrum, as well as thermodynamic properties of these models. The system of coupled quantum $S = \frac{1}{2}$ chains (spin-ladder) was found to behave differently depending on whether the number of chains is even or odd [1]. For an even number, the excitation spectrum is generically gaped and short-range correlations dominate in the ground state. The single $S = \frac{1}{2}$ quantum spin chain with dimerization exhibits quite similar properties, since it is known that dimerization produces an energy gap and destroys the quasi long-range order of the integrable uniform chain.

In a recent paper, Ref. [2], M.A. Martin-Delgado, R. Shankar, and G. Sierra have proposed a model of coupled spin chains with staggered dimerization which possesses a rich phase diagram, quite different from that of the simple spin ladder (no dimerization). Consider the simplest version of the model, containing two coupled $S = \frac{1}{2}$ Heisenberg chains (Fig. 1.):

$$H = J_\perp \sum_i \mathbf{S}_{1,i} \cdot \mathbf{S}_{2,i} + \sum_i \sum_{\alpha=1,2} J[1 + \delta(-1)^{i+\alpha}]\mathbf{S}_{\alpha,i} \cdot \mathbf{S}_{\alpha,i+1} \tag{1}$$

Here $\alpha = 1, 2$ is labeling the two chains (legs of the ladder). The coupling $J_\perp \geq 0$ is the inter-chain (rung) interaction and $J(1 \pm \delta) \geq 0$ are the nearest neighbor interactions along the chains (all couplings are antiferromagnetic). Notice that the dimerization $\delta$ is staggered in both directions (along and perpendicular to the chains), i.e. the dimerization in each chain is in antiphase with its neighbor chain. The model Eq.(1) was analyzed in Ref. [2] by mapping onto a non-linear sigma model (NLSM). In the NLSM approach the value of the topological angle $\theta$ determines the nature of the possible phases of the model [3]. For $\theta = 0$ the model is massive while it is massless for $\theta = $ (odd multiple of $\pi$). For the model at hand two massive (gaped) phases were found in the parameter plane $(\delta, J_\perp/J)$ with a massless (critical) line separating them, determined by the equation:

$$\theta = \frac{4\pi\delta}{2 + J_\perp/2J} = \pi \quad \Leftrightarrow \quad 4\delta = 2 + J_\perp/J \quad \text{(critical line)}. \tag{2}$$

A symmetric branch with $\delta \to -\delta$ ($\theta = 3\pi$) also exists but we will assume $\delta \geq 0$ from now on. The two massive phases separated by this line are basically phases where the dominant correlations are along the rungs or the stronger bonds along the legs. The existence of a critical line is quite unusual since individually both interactions, $J_\perp$ and $\delta$ are gap producing.

It is clear from Fig. 1. that there are two points $(\delta, J_\perp/J) = (0,0)$ and $(1,2)$ where the system is a single uniform chain and hence integrable and massless. The NLSM approach Eq.(2) does not correctly reproduce the point $(0,0)$ which is quite natural since it is expected to work in the vicinity of the point $(1,2)$ only. It has been conjectured in Ref. [2] essentially from continuity, that a critical line connects the two integrable points.

Let us mention that upon introducing an additional spin alternation [4] and (or) considering ladders of spin $S = 1$ or higher [2] the phase diagram of the system will be even more complex. The basic origin for this complexity however is still the staggered dimerization in the rung direction. Thus, form now on we will consider only the "minimal" model Eq.(1).

The purpose of the present work is to analyze the excitation spectrum and the phase diagram of the model Eq.(1) at $T = 0$ by a combination of numerical and analytical techniques. In Sec. II we present exact diagonalization results for the energy gap and the spin-spin correlations, confirming the existence of two gaped phases separated by a gapless line. In Sec. III we develop two kinds of strong-coupling approaches in the phase dominated by strong interchain (rung) correlations: (a) dimer series expansions, and (b) diagrammatic treatment of the effective Hamiltonian, written in terms of bond triplet operators. The spectrum near the critical line is calculated and the relevant interactions, responsible for the closing of the gap are identified. Sec. IV contains our conclusions and discussion of future prospects.

## II. EXACT DIAGONALIZATIONS

First we present results from finite lattice diagonalizations of the Hamiltonian Eq.(1), for systems of up to $N = 24$ spins. Periodic boundary conditions are used throughout. For reasons of symmetry the number of spins must be a multiple of 4, and most results are obtained from extrapolation of $12, 14, 16, 20, 24$ spin systems. We find empirically that the ground state is a singlet $S_{tot} = 0$ whereas the first excited state is a triplet $S_{tot} = 1$. The computed singlet-triplet gaps are extrapolated to the thermodynamic limit $N \to \infty$ via the ansatz:

$$\Delta E_N = \Delta E_\infty + \frac{A}{N} + \frac{B}{N \ln N} \tag{3}$$

where $A$ and $B$ are constants. The last term allows for the logarithmic corrections arising through conformal invariance in spin chains and effectively accounts for the residual curvature observed in direct ratio plots.

In Fig. 2. we show the variation of energy gaps versus the interchain coupling $J_\perp/J$ for various $N$, for a fixed value of the dimerization $\delta$ (in this case $\delta = \frac{1}{2}$). It is clear qualitatively that the variation in $\Delta E_N$ is small for both small and large values of $J_\perp/J$ whereas the variation is large near $J_\perp/J \approx 1.2$ where the individual curves have a minimum. The dashed lines, based on the extrapolated formula (3) clearly show the gap vanishing at a single point

on the $J_\perp/J$ axis. Similar results are obtained for other values of $\delta$ although for small $\delta$ the convergence is poorer. This is consistent with the increasing quantum fluctuations and larger finite size corrections expected near the uniform limit. This analysis leads to Fig. 3. which shows the estimated critical line in the $(\delta, J_\perp/J)$ plane. Comparing with Eq.(2) one can see that the NLSM result can not be trusted numerically, but the existence of a gapless line is correctly predicted.

In Fig. 4. we show various spin correlations versus $J_\perp/J$ for $\delta = \frac{1}{2}$. As intuitively expected the phase with $J_\perp/J > 1.22$ is characterized by strong inter-chain (rung) and weak intra-chain correlations. When $J_\perp/J$ decreases and ultimately crosses the critical point, the behavior of the correlation functions is reversed, signaling a transition into a phase, dominated by strong intra-chain correlations on the stronger bonds. We find that the spin correlations as well as the excitation gap change continuously through the quantum transition point.

## III. STRONG COUPLING EXPANSIONS

In this section we present analysis based on strong-coupling expansions around the limit $J_\perp \gg J$. Two approaches are used: the dimer series expansion and the bond operator mapping onto an effective interacting Bose gas. The two approaches are similar in spirit and produce quite similar result even though the technical details are different.

### A. Dimer series expansions

We start with results obtained by the linked-cluster dimer series expansion method. The linked-cluster expansion method has been previously reviewed in several articles [5–7], and will not be repeated here. The basic idea is to divide the Hamiltonian into two parts:

$$H = H_0 + V \tag{4}$$

where

$$H_0 = J_\perp \sum_i \mathbf{S}_{1,i} \cdot \mathbf{S}_{2,i},$$

$$V = J \sum_i \sum_{\alpha=1,2} [1 + \delta(-1)^{i+\alpha}] \mathbf{S}_{\alpha,i} \cdot \mathbf{S}_{\alpha,i+1} \tag{5}$$

By fixing values of $\delta$, we can construct an expansion in $J/J_\perp$ by taking $H_0$ as unperturbed Hamiltonian and $V$ as a perturbation. The zeroth order $V = J = 0$ approximation corresponds to isolated dimers (singlets) on the rungs. Each singlet can be excited into a triplet state and thus the excitation gap is $J_\perp$. Finite $J$ introduces interactions between the rungs

which modifies substantially the spectrum. In order to consider the physically interesting coupling region $J_\perp/J \sim 1$ the perturbation series has to be developed to high order and then extrapolated to the relevant point. We have carried out an expansion up to order $(J/J_\perp)^{23}$ for the ground state energy, to order $(J/J_\perp)^{13}$ for antiferromagnetic susceptibility, and to order $(J/J_\perp)^{11}$ for the triplet excitation spectra for several values of $\delta$. There are only 12 graphs that contribute to the ground state energy and dispersion, and 14 graphs that contribute to the antiferromagnetic susceptibility. The series coefficients are not presented here, but are available upon request. Then we have used integrated differential approximants and Padé approximants [8] to extrapolate the series. It is sometimes useful to compare the present results with the spectrum of a spin ladder without dimerization ($\delta = 0$), which can be found in Ref. [9] (see Fig. 4.).

In Fig. 5. we present the triplet excitation spectrum $\omega(k)$ for $\delta = \frac{1}{2}$, obtained by the dimer series expansions. The triplet gap $\Delta = \omega(\pi)$ decreases with the decrease of $J_\perp/J$, vanishing (within error bar) at the critical value $J_\perp/J = 1.23$. By comparing the spectra of Fig. 5. with the corresponding spectra for $\delta = 0$ (see Fig. 4. of Ref. [9] for the value $J_\perp/J = 2$) one can see that the renormalization due to finite $\delta$ is the strongest at $k = \pi$ while in the vicinity of the point $k = 0$ the energy is almost unrenormalized. This is due to the fact that the first three leading orders in $J/J_\perp$ do not change $\omega(k = 0)$ (see also Sec. III.B).

A more accurate determination of the critical line can be achieved by the Dlog Padé approximants to the antiferromagnetic susceptibility series, and the results are presented in Fig. 3. The phase boundary obtained within the dimer series approach is in excellent agreement with the exact diagonalization results in the region $J_\perp/J > 1$. For small values of $J_\perp$ the convergence of the dimer series becomes poorer (larger error bars), as the critical point occurs at much larger $J/J_\perp$. In Fig. 6. several critical spectra, for parameters on the massless line, are plotted. Notice that for $\delta = 1, J_\perp = 2J$ when Eq.(1) reduces to a "snake", i.e. one-dimensional Heisenberg chain, the dimer series reproduces correctly the spinon dispersion, which is known from the exact Bethe ansatz solution of the problem [10]. The latter is given by the formula (for a chain with exchange $J$): $\omega(k)/J = (\pi/2)\sin(\frac{\pi-k}{2})$. Indeed, the lower curve in Fig. 6. practically coincides with this formula.

Using the long series for the ground state energy, we were able to obtain the most accurate estimates of the ground state energy, as it was done before for the normal two-chain ladder [11]. For example for $\delta = 0.5$ and $J/J_\perp = 0.8$ which is near the critical line, the ground-state energy per site is estimated to be

$$E_0/NJ_\perp = -0.52655(2) \ . \tag{6}$$

Beside the above inter-chain dimer expansions about the limit $J_\perp \gg J$, we can also construct another dimer expansion, the intra-chain dimer expansion, by taking the stronger intra-chain bonds (the bonds couping $J(1+\delta)$) as unperturbed Hamiltonian, and the rest of

the bonds as perturbation, and carry out dimer series expansions in $(1-\delta)/(1+\delta)$ for fixed values of $J_\perp/J(1-\delta)$. The series have been computed up to order $[(1-\delta)/(1+\delta)]^{11}$ for the ground state energy, to order $[(1-\delta)/(1+\delta)]^6$ for the antiferromagnetic susceptibility, and to order $[(1-\delta)/(1+\delta)]^7$ for the triplet excitation spectra for several values of $J_\perp/J(1-\delta)$. With this expansion, one can study the excitation spectrum and the ground state properties for the parameters located within the intra-chain dimer phase. The gapless critical line derived from this expansion agrees well with that by inter-chain dimer expansions, but with much less accuracy. Here we will not present any detailed results from this dimer expansion, however the series are available upon request.

### B. Bond operator representation

In this section we describe a mapping of the model onto an interacting Bose gas, which can be achieved by using the bond operator representation for spins [12]. Denote by $|0\rangle_i$ the singlet state formed by two spins on rung $i$. Then, in the strong-coupling limit $J_\perp/J \gg 1$ the excitations are well described by triplets, created by the (bond) operators $t_{i,\alpha}^\dagger$, $|\text{triplet}\rangle_i = t_{i,\alpha}^\dagger |0\rangle_i$, where $\alpha = x, y, z$ are the three components of the triplet and the usual bosonic commutation relations hold [12]. The Hamiltonian Eq.(1) expressed in terms of the triplet operators is [13]:

$$
H = \sum_{i,\alpha,\beta} \left\{ J_\perp t_{\alpha i}^\dagger t_{\alpha i} + \frac{J}{2} \left( t_{\alpha i}^\dagger t_{\alpha i+1} + t_{\alpha i}^\dagger t_{\alpha i+1}^\dagger + \text{h.c.} \right) \right.
$$
$$
\left. + \frac{J}{2} \left( t_{\alpha i}^\dagger t_{\beta i+1}^\dagger t_{\beta i} t_{\alpha i+1} - t_{\alpha i}^\dagger t_{\alpha i+1}^\dagger t_{\beta i} t_{\beta i+1} \right) \right\} + H_\delta + H_U, \tag{7}
$$

where we have separated the part due to dimerization:

$$
H_\delta = \frac{\delta}{2} \sum_{i,\alpha,\beta,\gamma} (-1)^i \left\{ \left[ i\epsilon_{\alpha\beta\gamma} t_{\alpha i+1}^\dagger t_{\beta i}^\dagger t_{\gamma i} + \text{h.c.} \right] + [i \leftrightarrow i+1] \right\} \tag{8}
$$

and $H_U$ will be defined below. For $\delta = 0$ the Hamiltonian (7) coincides with that of the simple two-leg ladder [14,15]. In order for the triplet operators to represent only the physical spin triplet states, they have to satisfy the on-site hard-core constraint: $t_{\alpha i}^\dagger t_{\beta i}^\dagger = 0$. This restriction on the Hilbert space can be taken into account by introducing an infinite on-site repulsion between the triplets, as discussed in our previous work [15,16]:

$$
H_U = U \sum_{i,\alpha\beta} t_{\alpha i}^\dagger t_{\beta i}^\dagger t_{\beta i} t_{\alpha i}, \quad U \to \infty. \tag{9}
$$

Our goal is to develop a diagrammatic treatment of the interactions in the Hamiltonian (7) in order to understand which terms are most relevant to the renormalization of the spectrum. The quadratic part (first line in Eq.(7)) is diagonalized in momentum space by a

6

Bogoliubov transformation $t_{\alpha k} \to u_k t_{\alpha k} + v_k t_{\alpha-k}^\dagger$, which leads to the spectrum $\omega_k^2 = A_k^2 - B_k^2$, with $A_k = J_\perp + J\cos(k)$, $B_k = J\cos(k)$. The Bogoliubov coefficients are defined as: $u_k^2, v_k^2 = \pm 1/2 + A_k/2\omega_k$.

The spectrum of the Hamiltonian Eq.(7) without the dimerization term $H_\delta$ was investigated diagrammatically in Refs. [15,16]. Here we only summarize the results. The on-site repulsion $H_U$ gives the dominant contribution to the spectrum renormalization, while the two-particle inter-site interaction with strength $J/2$ (first term in the second line of Eq.(7)) is a relatively minor effect [17]. Even though the on-site interaction is infinite, the scattering amplitude $\Gamma_{\alpha\beta,\gamma\delta}(k,\omega) = \Gamma(k,\omega)(\delta_{\alpha\gamma}\delta_{\beta\delta} + \delta_{\alpha\delta}\delta_{\beta\gamma})$ is finite (as physically expected), which can be seen by resumming the ladder series, shown in Fig. 7(a) and setting $U \to \infty$. The scatering amplitude and the corresponding self-energy (Fig. 7(b)) are [15,16]:

$$[\Gamma(k,\omega)]^{-1} = \sum_q \frac{1}{-\omega + \omega_q + \omega_{k-q}} \ , \ \Sigma_U(k,\omega) = 4\sum_q v_q^2 \Gamma(k+q, \omega - \omega_k). \tag{10}$$

Here, and in all future equations we set, for convenience, the number of rungs to unity. As emphasized in Ref. [15,16], Eq.(10) represents the dominant contribution from $H_U$, provided the density of triplets $N_t = \langle t_{\alpha,i}^\dagger t_{\alpha,i}\rangle = 3\sum_q v_q^2$ is small. Thus Eq.(10) should be viewed as the first term in an expansion in powers of $N_t$. For the simple ladder ($\delta = 0$) we find (after solving the corresponding Dyson equation, see below) $N_t \approx 0.1$ for $J_\perp = 2J$, and $N_t \approx 0.25$ for $J_\perp = J$. Therefore the dilute gas approximation is expected to work quite well even for $J_\perp/J \sim 1$. Naturally when $J_\perp/J \to 0$ the above picture, based on strong rungs, breaks down. Instead, the excitations in this regime should be viewed as weakly bound spinons, thus making the local triplets an inadequate staring point. We have estimated that the bond operator formalism describes well the excitation spectrum for $J_\perp/J > 1$ [15,18].

Next we turn to the three-particle term $H_\delta$ which represents the dimerization part of the Hamiltonian. To lowest (one-loop) order there are contributions to the normal and anomalous self-energies, drawn in Fig. 7(c) and Fig. 7(d), respectively. The corresponding formulas are:

$$\Sigma_\delta^N(k,\omega) = 4(\delta J)^2 \sum_q \frac{[C(q+\pi, k-q, k)]^2}{\omega - \omega_{q+\pi} - \omega_{k-q}} + \left\{ \begin{array}{c} u \leftrightarrow v \\ \omega \to -\omega \end{array} \right\}, \tag{11}$$

$$\Sigma_\delta^A(k,\omega) = 4(\delta J)^2 \sum_q \frac{C(q+\pi, k-q, k)D(q+\pi, k-q, k)}{\omega - \omega_{q+\pi} - \omega_{k-q}} + \left\{ \begin{array}{c} u \leftrightarrow v \\ \omega \to -\omega \end{array} \right\}, \tag{12}$$

where the following definitions are used

$$C(k,p,q) = \Phi(k,p)u_k u_p + \Phi(-q,p)u_k v_p + \Phi(k,-q)v_k u_p, \tag{13}$$

$$D(k,p,q) = -C(k,p,q)\{u \leftrightarrow v\}, \Phi(k,p) = \frac{1}{2}(\sin k - \sin p). \tag{14}$$

7

The function $\Phi(k, p)$ originates from the Fourier transform of the three-particle vertex Eq.(8). Equations (11) and (12) can be derived by evaluating all possible internal loops in the diagrams in Figs. 7(c),(d), where, as usual, lines with a single arrow stand for the normal Green's function $G^N(k, t) = -i\langle Tt_{\alpha,k}(t)t^\dagger_{\alpha,k}(0)\rangle$ and lines with double arrows represent the anomalous Green's functions $G^A(k, t) = -i\langle Tt^\dagger_{\alpha,-k}(t)t^\dagger_{\alpha,k}(0)\rangle$. Finally, the coupled Dyson's equations for the normal and anomalous Green's functions have to be solved leading to the result (more details can be found in [18]):

$$G^N(k,\omega) = \frac{\omega + A_k + \Sigma^N(k,-\omega)}{[\omega + A_k + \Sigma^N(k,-\omega)][\omega - A_k - \Sigma^N(k,\omega)] + [B_k + \Sigma^A(k,\omega)]^2}, \tag{15}$$

where the total normal and anomalous self-energies are defined as

$$\Sigma^N(k,\omega) = \Sigma_U(k,\omega) + \Sigma_\delta^N(k,\omega), \quad \Sigma^A(k,\omega) = \Sigma_\delta^A(k,\omega). \tag{16}$$

In order to get a feeling for the effect of $H_\delta$ on the spectrum, it is instructive to examine the second order perturbation theory result. It can be obtained by noticing that to leading order $\omega_k \approx J_\perp, u_k \approx 1, v_k \approx -(J/2J_\perp)\cos k$. Thus in evaluating the leading order correction arising from the dimerization term one can set $v_k = 0$ which means that only the normal self-energy contributes:

$$\delta\omega_k = \Sigma_\delta^N(k,\omega_k) = 4(\delta J)^2 \sum_q \frac{\Phi^2(q + \pi, k - q)}{-J_\perp} = \frac{\delta^2 J^2}{J_\perp}(\cos k - 1). \tag{17}$$

One can see that to lowest order the renormalization of the spectrum for $k = \pi$ is the strongest while $k = 0$ is not renormalized. For a fixed value of $\delta$, the gap $\omega(\pi)$ decreases with decreasing $J_\perp/J$ and vanishes at a critical ratio, signaling an instability of the rung dimer phase.

We have found the spectrum numerically by solving for the poles of the exact Green's function Eq.(15), thus resumming the perturbation series to all orders. The results for $\delta = \frac{1}{2}$ are presented in Fig. 5. The diagrammatic results are in good agreement with the dimer series expansions, however with decreasing $J_\perp/J$ the disagreement increases. We would like to point out that even though the two methods have the same starting point (strong rungs) and typically agree quite well in the region of strong coupling, for smaller coupling the dimer series expansion performs better. The reason is that the series expansion takes into account all terms to a particular (finite) order, while the diagrammatic approach sums up only the most dominant subclass of diagrams. The small parameter $N_t$ controlling the diagrammatic expansion grows with decreasing $J_\perp/J$ and at $J_\perp = 1.23J$ (the critical point, as estimated by the dimer series and exact diagonalization) has the value $N_t = 0.3$. This relatively large value of the triplet density is related to the considerably decreased magnitude of the spin-spin correlation function on the rungs [19] (see the (1,2) correlations in Fig. 4.). Therefore the agreement between the diagrammatic analysis and the dimer series is, in fact, even better than expected.

## IV. SUMMARY AND DISCUSSION

In conclusion, we have investigated the excitation spectrum and the ground state phase diagram of the quantum spin ladder with staggered dimerization and have found that a transition takes place form a phase dominated by strong rung correlations into a phase, characterized by intrachain dimers. The two phases are separated by a gapless line. The location of the boundary, the triplet excitations, as well as the spin-spin correlations in the rung dimer phase were calculated by dimer series expansions, diagrammatic analysis of the effective hard-core Bose gas of rung triplets, and exact diagonalizations.

We have identified the three-particle scattering $H_\delta$, in terms of the rung triplets, to be responsible for the instability of the rung dimer phase (closing of the gap). It is interesting to note that this is indeed the term which, in the continuous field theory formulation, contributes to the topological angle $\theta$ and leads to the transition. Indeed, from the representation of the spin operator on a given rung $i$ in terms of the triplets [13] one can easily see that $\mathbf{S}_1 - \mathbf{S}_2 \sim \mathbf{t}_i + \mathbf{t}_i^\dagger \sim \boldsymbol{\phi}_i$, $\mathbf{S}_1 + \mathbf{S}_2 \sim i\mathbf{t}_i^\dagger \times \mathbf{t}_i \sim \mathbf{l}_i$. These are precisely the two vector fields used in the derivation of the non-linear sigma model [3]. Therefore the terms of the form $\boldsymbol{\phi}_i \cdot \mathbf{l}_{i+1}$ which appear in our lattice Hamiltonian $H_\delta$ would be precisely the ones which give a non-trivial $\theta$ after the continuum limit is taken.

There are several additional aspects of the problem that can be addressed within the strong-coupling formalism described in this paper. As suggested in Ref. [2] the spinons become unconfined on the gapless line separating the two phases of the model (see Fig. 3.). Since in the two massive phases confinement definitely takes place, we would expect that the triplet spectral weight decreases as the critical line is approached and ultimately goes to zero. In addition, at the point of deconfinement the same energy is required to create triplet and singlet excitations. Therefore, close to the critical line, a low-energy singlet excitation must appear in the spectrum. Within the strong-coupling approach a singlet can be viewed as a collective bound state of two triplets [15]. While in the spin ladder without dimerization the singlet bound state is high in energy (small binding energy), in the present model we expect it to become a truly low-energy state (strong triplet binding). We leave these issues for a future study [20].

While this manuscript was being prepared for publication we became aware of two recent preprints devoted to the same model [21]. Both of these works have studied the phase diagram numerically via exact diagonalization and their results for the location of the critical line are in agreement with ours.

## ACKNOWLEDGMENTS

# REFERENCES

$^{\dagger}$     Address after Dec. 10, 1998: Department of Physics, University of Florida, Gainesville, FL 32611-8440; e-mail: valeri@phys.ufl.edu

$^{\ddagger}$     e-mail: otja@newt.phys.unsw.edu.au

$^{*}$     e-mail: zwh@newt.phys.unsw.edu.au

[1] See e.g. the review: E. Dagotto and T.M. Rice, Science **271**, 618 (1996).

[2] M.A. Martin-Delgado, R. Shankar, and G. Sierra, Phys. Rev. Lett.**77**, 3443 (1996).

[3] For a review of the NLSM approach, see: I. Affleck, in *Fields, Strings, and Critical Phenomena*, edited by E. Brezin and J. Zinn-Justin (North-Holland, Amsterdam, 1989), p.565; G. Sierra, cond-mat/9610057 (unpublished).

[4] T. Fukui and N. Kawakami, Phys. Rev. B **57**, 398 (1998); A. Koga, S. Kumada, N. Kawakami, and T. Fukui, J. Phys. Soc. Jpn. **67**, 622 (1998).

[5] H.X. He, C.J. Hamer and J. Oitmaa, J. Phys. A **23**, 1775(1990)

[6] M.P. Gelfand, R.R.P. Singh, and D. Huse, J. Stat. Phys. **59**, 1093 (1990).

[7] M. P. Gelfand, Solid State Commun. **98**, 11(1996).

[8] A.J. Guttmann, in *Phase Transitions and Critical Phenomena*, edited by C. Domb and J. Lebowitz (Academic, New York, 1989), Vol. 13.

[9] J. Oitmaa, R.R.P. Singh, and W.H. Zheng, Phys. Rev. B **54**, 1009 (1996).

[10] J. des Cloizeaux and J.J. Pearson, Phys. Rev. **128**, 2131 (1962); L.D. Faddeev and L.A. Takhtajan, Phys. Lett. A **85**, 375 (1981).

[11] W.H. Zheng, V.N. Kotov, and J. Oitmaa, Phys. Rev. B **57**, 11439 (1998).

[12] A.V. Chubukov, JETP Lett. **49**, 129 (1989); S. Sachdev and R. Bhatt, Phys. Rev. B **41**, 9323 (1990).

[13] The spin operators are related to the triplet operators via the transformation [12]: $S^{\alpha}_{(1,2),i} = 1/2(\pm t^{\dagger}_{\alpha i} \pm t_{\alpha i} + i\epsilon_{\alpha\beta\gamma}t^{\dagger}_{\beta i}t_{\gamma i})$, $\alpha = x, y, z$.

[14] S. Gopalan, T.M. Rice, and M. Sigrist, Phys. Rev. B **49**, 8901 (1994); R. Eder, Phys. Rev. B **57**, 12832 (1998).

[15] O.P. Sushkov and V.N. Kotov, Phys. Rev. Lett. **81**, 1941 (1998).

[16] V.N. Kotov, O.P. Sushkov, W.H. Zheng, and J. Oitmaa, Phys. Rev. Lett. **80**, 5790 (1998).

[17] To lowest (one-loop) order, this term leads to the renormalization [15]: $A_k \rightarrow A_k + 2J\sum_q v_q^2 \cos q$, $B_k \rightarrow B_k - 2J\sum_q v_q u_q \cos q$, which is understood in all formulas in the text.

[18] V.N. Kotov, O.P. Sushkov, and R. Eder, to appear in Phys. Rev. B, 1 March (1999); cond-mat/9808169.

[19] The spin-spin correlations on the rungs are related to the triplet density via: $\langle \mathbf{S}_1 \cdot \mathbf{S}_2 \rangle = -3/4 + N_t$, and thus from Fig. 4. at the point $J_{\perp} = 1.23J$ we can estimate $N_t \approx 0.37$.

[20] V.N. Kotov and J. Oitmaa (unpublished).

[21] D.C. Cabra and M.D. Grynberg, cond-mat/9810263 (unpublished); M.A. Martin-Delgado, J. Dukelsky, and G. Sierra, cond-mat/9810379 (unpublished).

# FIGURES

FIG. 1. The spin ladder with staggered dimerization.

FIG. 2. Energy gap for different system sizes (solid lines) and its extrapolation to the thermo-dynamic limit (dashed line).

FIG. 3. Phase diagram of the model. Open circles are the exact diagonalization data, where the circle diameter represents the error in the determination of the critical point. Solid squares with error bars are the critical points obtained by Dlog Padé approximation of the dimer series.

FIG. 4. Spin-spin correlations $\langle S_i^z S_j^z \rangle$ (where (i,j) are defined in Fig. 1.) obtained by exact diagonalization of a system of $N = 20$ spins. The dashed line represents the location of the critical point.

FIG. 5. Triplet energy spectrum obtained by the dimer series expansion (solid squares connected by solid lines) for $J_\perp/J = 2, 1.43, 1.23$ (upper, lower and middle curve at $k = \pi$, respectively). The corresponding spectra, obtained from the poles of Eq.(15) are drawn, respectively, with solid, long-dashed and short-dashed lines.

FIG. 6. Same as Fig.5. for several values of $(\delta, J_\perp)$ on the gapless line.

FIG. 7. (a) Resummation of the ladder series for the scaterring amplitude $\Gamma(k, \omega)$, where $k(\omega)$ is the total incoming momentum (energy), $k = k_1 + k_2$. (b) The normal self-energy corresponding to $\Gamma$. (c) Lowest order diagrams for the normal self-energy arising from the three-particle term $H_\delta$. (d) Same as (c) for the anomalous self-energy. The dots represent all other possible diagrams with different internal loops.
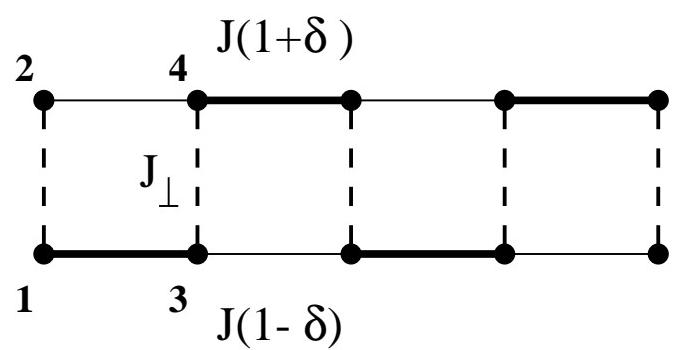
FIG.1.
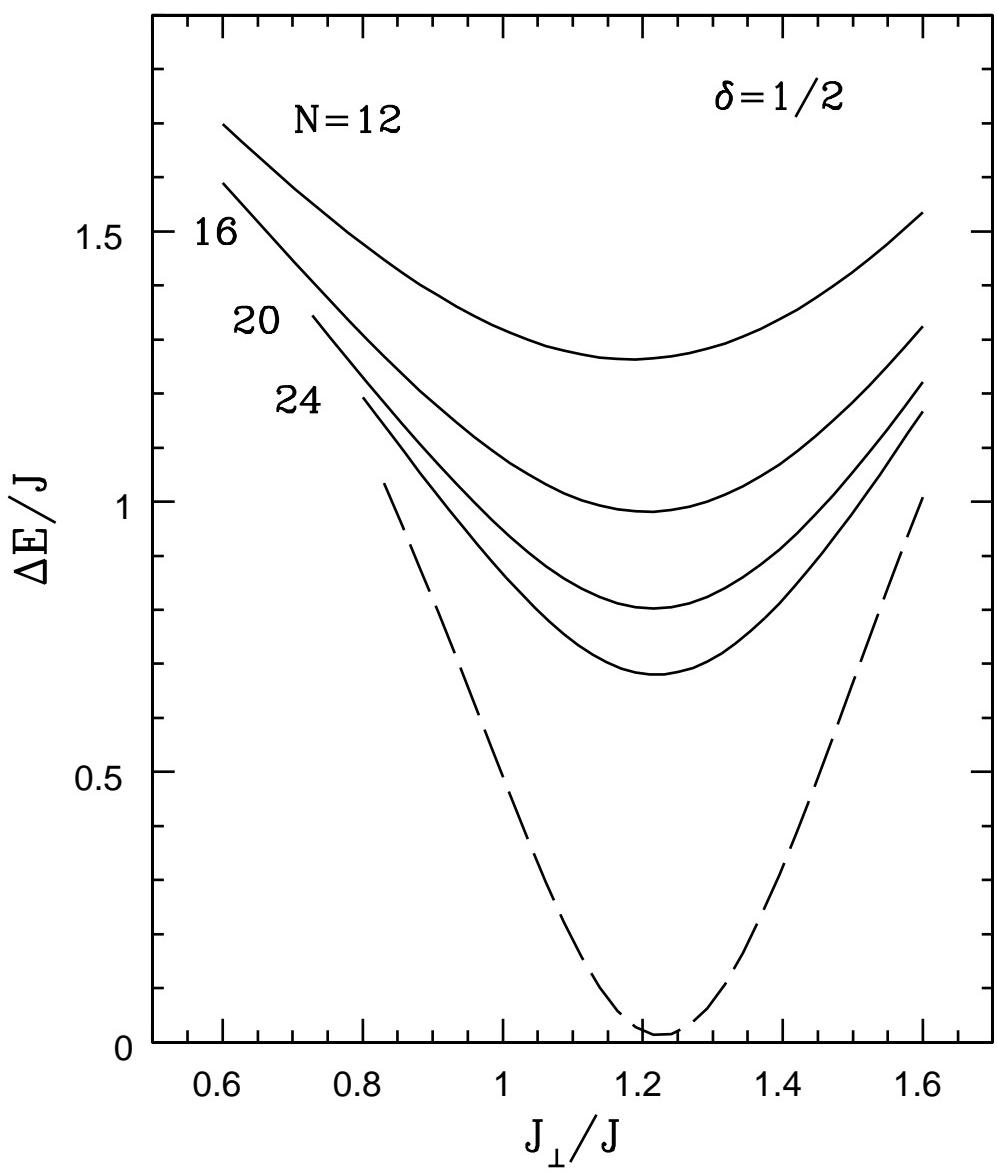
FIG.2.
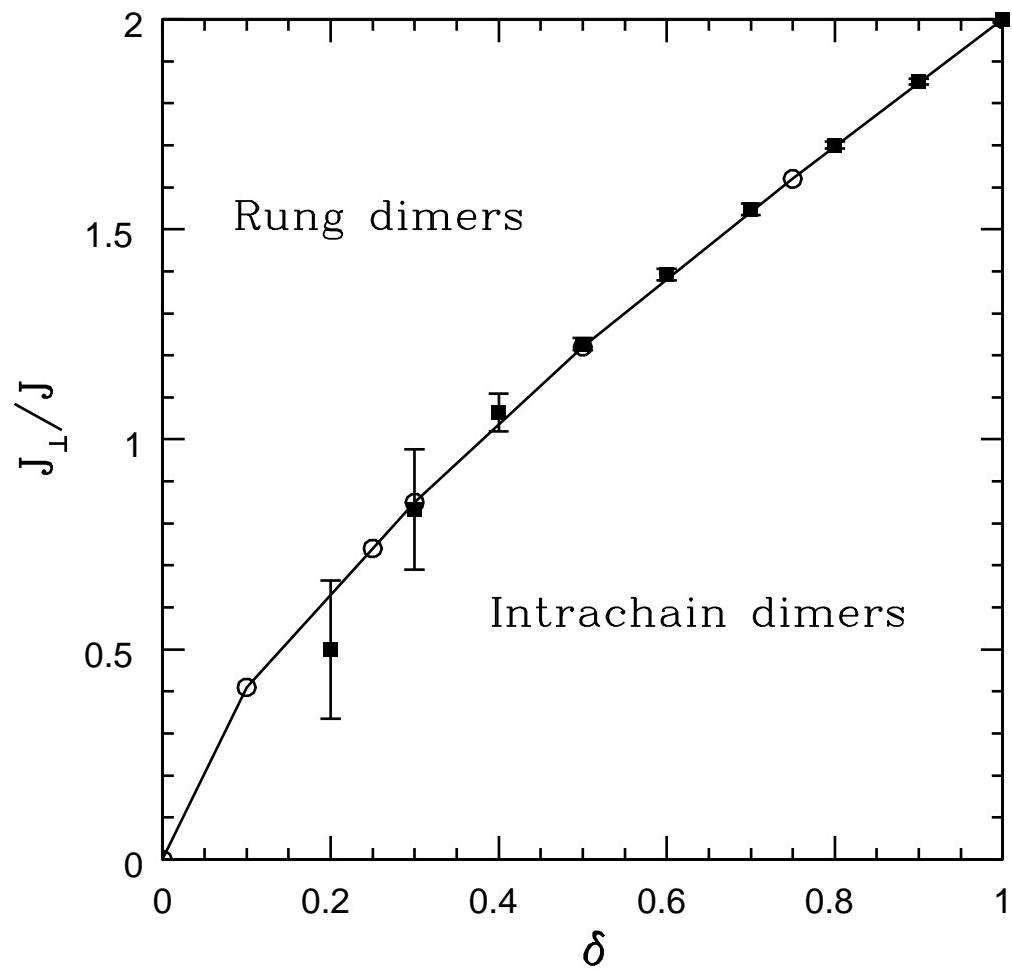
FIG.3.

FIG.4.

FIG.5.

FIG.6.

**(a)**



**(b)**



**(c)**



**(d)**



**FIG.7.**